



All Student Publications

---

2017-08-18

# Developing Instrumentation for Fabricating and Characterizing Thin Film Aluminum Mirrors

P. Claire Segura  
psegura@oberlin.edu

Follow this and additional works at: <https://scholarsarchive.byu.edu/studentpub>

 Part of the [Astrophysics and Astronomy Commons](#)

This paper was completed during the 2017 Research Experiences for Undergraduates in Physics (REU) program. More information about this program can be found [here](#).

---

## BYU ScholarsArchive Citation

Segura, P. Claire, "Developing Instrumentation for Fabricating and Characterizing Thin Film Aluminum Mirrors" (2017). *All Student Publications*. 213.

<https://scholarsarchive.byu.edu/studentpub/213>

This Report is brought to you for free and open access by BYU ScholarsArchive. It has been accepted for inclusion in All Student Publications by an authorized administrator of BYU ScholarsArchive. For more information, please contact [scholarsarchive@byu.edu](mailto:scholarsarchive@byu.edu), [ellen\\_amatangelo@byu.edu](mailto:ellen_amatangelo@byu.edu).

# Developing Instrumentation for Fabricating and Characterizing Thin Film Aluminum Mirrors

P. Claire Segura

Advisor: R. Steven Turley

2017 REU

August 18, 2017

## Abstract

The best material for constructing a mirror for a broad-bandwidth telescope that is also capable of reflecting EUV light is pure aluminum. In order to test how the reflectance of aluminum in the EUV range changes as it oxidizes, a system has been constructed that allows a thin aluminum mirror to be constructed inside of a vacuum, where its reflectance can then be tested immediately. Because the experiment must take place in a vacuum, it must also be controlled remotely through a computer program, which manages the mirror fabrication process as well as the collection and analysis of reflectance data. This data analysis process accounts for other factors that influence the measured intensity of the reflected light aside from the surface of the mirror and the angle of incidence, including the position of the detector, random noise, and the time dependence of the plasma source. This ensures that the actual reflectance of the mirror at a given angle of incidence is always clearly distinguishable in the data. The fabrication controls are now at a stage where they can be used to create a mirror inside the chamber of the reflectometer. A separate part of the program is currently in use to scan the detector across the beam and perform several calculations using the resulting data. Once the most consistent method of analysis is determined, this method will be implemented as part of the main program, which will then be ready for testing with the experimental equipment.

## Contents

<b>1</b>	<b>Introduction</b>	<b>1</b>
<b>2</b>	<b>Equipment</b>	<b>3</b>
<b>3</b>	<b>Fabrication Controls</b>	<b>4</b>
<b>4</b>	<b>Data Collection</b>	<b>5</b>
4.1	Concerns for Analysis	5
4.2	Development of the Data Analysis Code	6
<b>5</b>	<b>Milestones</b>	<b>8</b>
<b>6</b>	<b>Future Plans</b>	<b>9</b>

# 1 Introduction

Extreme ultraviolet light refers to the portion of the electromagnetic spectrum between about 20 to 100 nm. EUV light is particularly useful in the field of astronomy since a major part of astronomical knowledge depends on spectroscopic analysis, a technique that is limited by the range of wavelengths that can be detected by telescope. In the past, NASA's IMAGE mission used the 30.4 nm EUV light scattered from singly ionized helium trapped in Earth's magnetosphere to study this area beyond our atmosphere, producing images that allow astronomers to gather new information about Earth's magnetic field [1]. A more powerful telescope could look beyond Earth and search for magnetospheres of distant exoplanets. The short wavelength of EUV light also means that it scatters well off of atmospheric atoms and molecules, making it a useful tool for detecting and characterizing exoplanet atmospheres [2].

It is clear that outfitting the next large, space based telescope with a mirror capable of reflecting EUV light will be an important advancement in astronomy, but not if it comes at expense of the telescope's ability to detect other wavelengths, such as infrared and visible light. An ambitious space-based telescope, such as the Large UV/Optical/Infrared Surveyor (LUVOIR) that will be under consideration at NASA's 2020 decadal survey [3], must be able to gather as much information as possible in a wide range of wavelengths. Extending the capabilities of such a telescope into the EUV is a major challenge, because very few materials will reflect light well in the EUV range. Mirrors exist that have been designed specifically for EUV reflection, but they do not reflect well at longer wavelengths. It is necessary to develop a new mirror design, one that is capable of reflecting light from infrared to extreme ultra violet wavelengths.

By far the best design for such a broad bandwidth mirror is a thin layer of pure aluminum above a mirror designed specifically to maximize EUV reflectance. Figure 1 shows the computed reflectance of pure aluminum using values for the index of refraction from IMD [4]. Aluminum has a reflectance of 90% at wavelengths greater than 89 nm. The reflectance begins to drop at about this point, and aluminum is no longer reflective about 85nm (15ev) [1]. This is aluminum's plasma frequency, and it is related to the number of free electrons in the surface of a reflective metal. Aluminum's plasma frequency is higher than that of most metals, allowing it to reflect a larger bandwidth of light [1]. At higher frequencies, aluminum becomes transparent, allowing a reflective EUV mirror placed beneath the aluminum layer to extend the bandwidth of the mirror beyond 85 nm and into the EUV.

There is, however, a major challenge to creating a first-surface aluminum mirror. The same free electrons that make aluminum such a useful reflector also attract oxygen, and so aluminum oxidizes quickly when it is exposed to air. Figure 2 shows a computation of how aluminum's reflectance changes as the thickness of the oxide layer increases, also using the index of refraction from IMD [4]. It is clear that aluminum loses its strong reflectance at high wavelengths. Aluminum oxide also absorbs UV light, preventing it from penetrating to the layers beneath. Our goal is to investigate this effect experimentally by creating thin film aluminum mirrors in a vacuum, and measuring the reflectance and oxidation to gather information that will be beneficial in guiding the development of mirrors for large aperture telescopes.

# 2 Equipment

All of the physical pieces are in place to fabricate an aluminum mirror and test its reflectance. The setup for testing reflectance consists of three main parts: a hollow cathode plasma source, a monochromator, and a reflectometer (see figure 3).

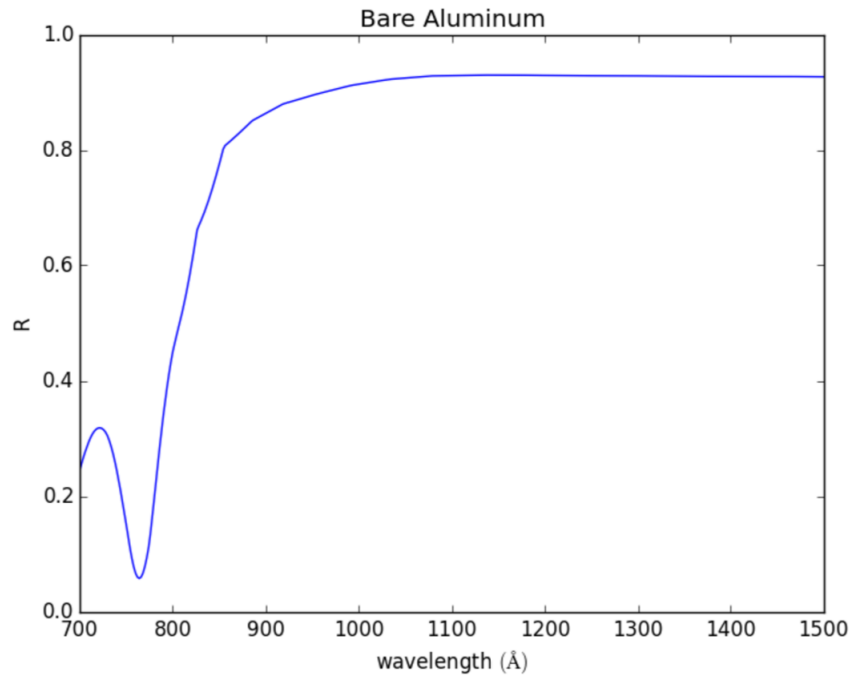


Figure 1: Calculated reflectance of bare aluminum [2].

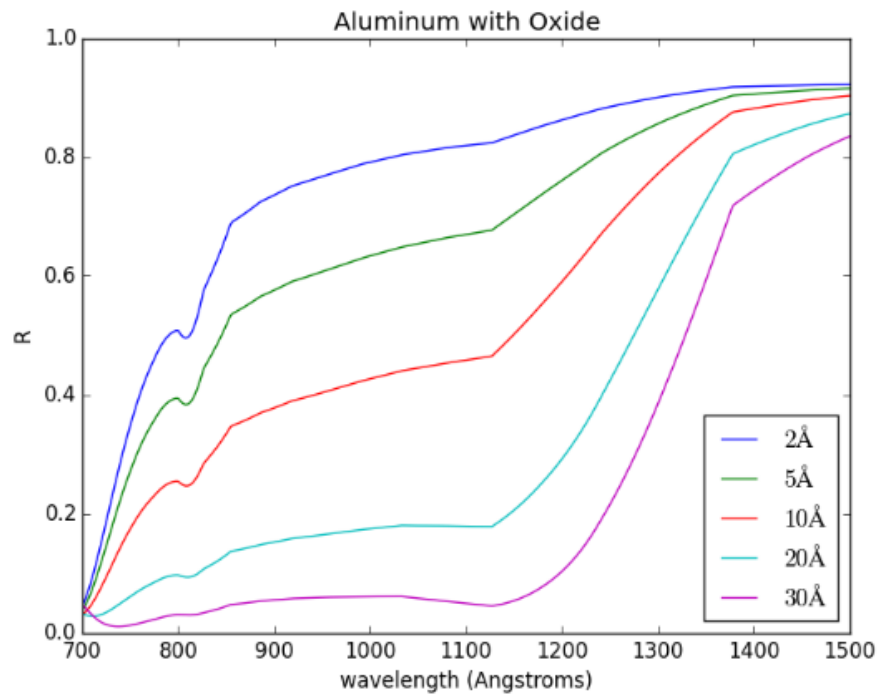


Figure 2: Calculated reflectance of aluminum coated with aluminum oxide. Each curve represents a different thickness of the aluminum oxide layer [2].

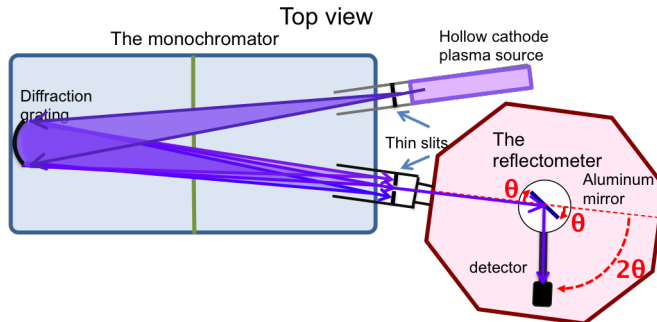


Figure 3: A top view of the equipment used for testing the reflectance of the aluminum sample.

The hollow cathode serves as the source of EUV light. Inside the hollow cathode, gas flows through the cavity, and the strong electric field pulls the electrons off some of the molecules, creating a plasma of ions and free electrons. The electrons are accelerated towards the ground side of the chamber. When a free electron collides with an ion, energy is imparted to the ion, which can excite the ion's electrons to higher energy states. When the electrons decay, photons are emitted at the specific transition wavelength. The set of possible transitions is unique to a particular element, so by selecting a certain gas to use in the chamber, one can also select a unique group of frequencies at which light is emitted.

From this group a single wavelength is selected by the monochromator. Light enters the monochromator through a slit and reflects off of a diffraction grating, which causes light at different frequencies to focus at distinct points. By focusing only the desired wavelength on the small exit slit, the grating ensures that only the desired wavelength is passed into the reflectometer.

The reflectometer is an octagonal structure containing the sample and the detector. The sample aluminum mirror can rotate to adjust the angle of incidence, and the detector is attached to an arm that allows it to revolve around the sample. In order to ensure that the light from the sample is reflected completely into the detector, the angle of the detector relative to the beam is kept at twice the angle of the sample relative to grazing incidence. The detector measures the intensity of the light, which allows us to determine the reflectance of the sample.

The fabrication process takes place inside the reflectometer, where a five-walled box containing a tungsten filament and a small piece of aluminum foil is mounted from the roof of the chamber on a movable arm (see figure 4). When the time comes to create an aluminum mirror, the box will move into position over a silicon substrate. A current travels through the filament, heating it up until the aluminum vaporizes, coating the silicon substrate with a thin layer of aluminum. When the box is removed, an aluminum mirror has been created that has not yet been exposed to oxygen, and it is ready to be tested in the reflectometer.

Each step of the process must be controlled remotely through a computer program. The focus of the work done this summer has been in writing and developing various parts of the program, both for the fabrication of the mirror and testing the reflectance.

### 3 Fabrication Controls

The evaporation process brings the tungsten filament to a specified target resistance. The user specifies this resistance and also gives values for the resistance when the voltage is at 4V and when it is at 6V, which are used to interpolate a value for the target voltage. When

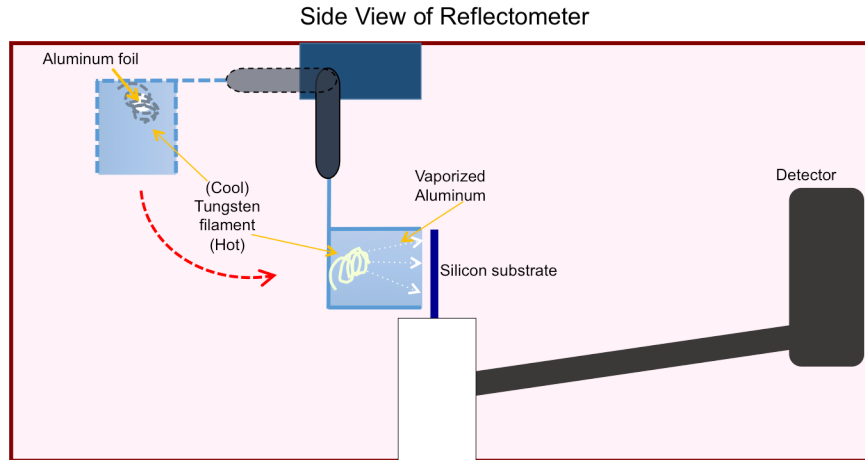


Figure 4: A side view of the chamber of the reflectometer demonstrating the fabrication process.

the program is first started, the voltage is set to its maximum value (6V), and once the current reaches 88 Amps it switches to the target voltage. When the program is stopped or a time of 15 seconds has passed, the voltage returns to 0, and the aluminum now coats the surface of the mirror. This process has been successfully used to fabricate an aluminum mirror, which has not yet been tested for uniformity and thickness. From a programming perspective, the fabrication process is complete, and the focus has moved to developing the code needed to test the reflectance of a fabricated sample.

## 4 Data Collection

### 4.1 Concerns for Analysis

The primary influence on how the data collection process is currently being designed is the fact that the intensity read by the detector at any given instant is influenced by 4 major factors, three of which have no relationship to the reflectance of the aluminum and so should be accounted for automatically by the program. These four factors are: the angle of incidence of the beam on the sample, random noise, the position of the beam relative to the opening of the detector, and the time dependence of the plasma source.

The dependence on the angle of the sample is the quantity that the experiment is designed to measure, therefore its effect needs to be clearly visible in the data and distinguishable from any of the other factors.

There are three main sources of random noise: the plasma, the electronics, and the detector. A photon is produced from the plasma when an electron collides with an ion in the chamber of the hollow cathode. This is a random event that does not occur in regularly spaced intervals, so there will always be some random fluctuations in the intensity of the beam. Density fluctuations and turbulence in the plasma also contribute to the random noise associated with the plasma source. The electronic noise is an unavoidable part of any electronic measurement. The noise from the detector is related to the randomness of photon production and reflection. The detector counts the number of photons that enter in a certain time period, because photon production is a random event, this detector reading will fluctuate as well.

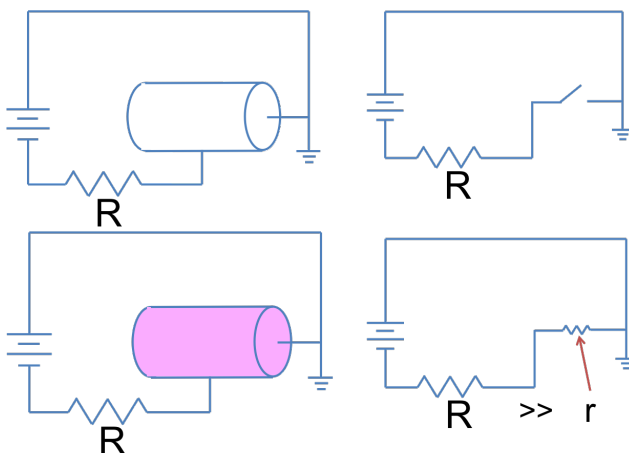


Figure 5: When the plasma is unlit (top), the hollow cathode acts as a break in the circuit. When the plasma is lit (bottom), its resistance is very small, so a ballast resistor is included to control the current.

The beam of light coming from the plasma source is larger than the aperture of the detector, so the intensity reading from the detector will depend on what part of the beam is read. The motors that control the position of the detector are not precise enough to ensure that the detector is positioned at the same part of the beam every time it is re-positioned. Even if it could be placed at the same point, the fluctuations of the plasma source cause the intensity to vary randomly across the beam, so the brightest point is not always in the same place.

The hollow cathode is connected to a high voltage source, and since the cathode has a very low resistance once the plasma is lit, it is necessary to limit the current through the system by connecting it in series with a ballast resistor (see figure 5). However, as a resistor heats up, its resistance increases, and since the voltage is constant, the current will decrease. Thus the same property that we take advantage of for the evaporator causes problems as we attempt to measure the reflectance of the sample. As the current through the plasma source decreases, the intensity of the light it produces decreases as well. This means that the intensity of the light incident on the reflected sample will decrease with time. If this remains un-accounted for, the reflectance will appear to decrease as the scan continues, giving an inaccurate picture of how the reflectance is actually changing with the angle.

## 4.2 Development of the Data Analysis Code

Each factor affects the data on a different scale, so by focusing on a single step in the data collection process where all but one factor has a negligible effect, we can counter the effects of that single factor. These steps are determined in a specific order, so each step is able to implement what was learned in the previous step to ensure that only a single factor is visible in the process. In the end, all of the individual pieces will be put together in a single, automated scanning process.

The process starts at the level of a single measurement on the detector, where the primary influence is the random noise from the detector. The detector works by counting the number of photons that enter in a specified time span, so allowing the user to specify how long the detector counts every time it takes a measurement allows the noise to be minimized. The detector reports its value in photons per second, so the longer the detector spends counting photons, the less influence random fluctuations in the photon count have

on the final value. However, there is a trade-off involved with this step, as the longer the detector takes to count, the more likely it is that the time dependence of the plasma source will have a non-negligible impact on the intensity of the beam. Allowing the user to adjust this time ensures that the time spent on a single count can be optimized to suit the needs of a given situation.

The next step is to investigate the dependence on the position of the detector with respect to the beam. In this process, the sample is put at a single angle (or moved out of the way of the beam), and the detector is moved across the beam, stopping at regular intervals to take a measurement (see figure 6). The time that it takes for the detector to scan across this angle should be short enough that the time dependence of the plasma source is negligible. The same trade-off that determines the length of time spent counting for a single point also applies to the detector scan: the more data points are taken, the better the scan represents the intensity of the beam, but the more time it will take for the scan to complete. The ultimate goal for this process is to reduce the detector scan to a single value for the count and the time, which we can then use as a representative value for the intensity of the beam. The best method for doing this task has not yet been decided, so the program automatically performs several different calculations, the results of which are displayed on the screen in figure 6. These methods include fitting the entirety of the data to a Lorentzian and Gaussian curve and determining the center position and amplitude of that curve, as well as repeating this process with a small section of the data between two cursors that can be positioned by the user. Once the appropriate method of determining a count has been found experimentally, this method will be implemented for every data point collected in the future so the intensity value of each data point is one that does not depend on variations in the angle of the detector.

The process that accounts for the time dependence of the plasma source has been designed and implemented as part of the program known as the  $\theta - 2\theta$  scan process (after the relationship between the angle of the sample and the angle of the detector), which will eventually serve as the final compilation of all the previously discussed analysis methods, and serve as the main program used for data collection. In this process, the sample is moved from a minimum angle to a maximum angle, stopping at regular intervals to scan the detector across the beam and calculate the reflectance, which is displayed on a graph as a function of the position of the sample. The reflectance is determined from the ratio of the light reflecting off the sample ( $I$ ) to the light traveling directly into the detector ( $I_0$ ). As a scan continues, at regular intervals the detector and sample move back to the zero position, and the sample moves out of the way so that the detector can read the intensity of the light ( $I_0$ ) that is coming straight from the plasma source, and record this value along with its associated time. The sample and detector then move back past to previous locations, and continue to the next angle in the scan. In between intensity points, the program will determine two data points of intensity reflected from the sample, and records the counts, sample angle, and time of each point. Once at least two  $I_0$  measurements have been taken, the program constructs a polynomial fit between the points, and stores the coefficients that represent the function of  $I_0$  with respect to time. When the next reflected intensity data point is taken, the program automatically uses these coefficients to extrapolate  $I_0$  at the time of the new point, and to interpolate  $I_0$  at the time of every previously taken reflected data point. The reflectance at each point is recalculated ( $I/I_0$ ), and the graph is updated to display the new reflectance with respect to position. In this way, the fit improves as more intensity points are taken and the reflectance is recalculated with respect to interpolated  $I_0$ . At the end of the scan, a final  $I_0$  measurement is taken, and the entire set of  $I_0$  points are fit a final time. This fit is used to interpolate  $I_0$  at the time of every reflected  $I$  data point. The reflectance is recalculated, and the graph is updated to show reflectance as a function of position. At this point the data has been normalized to account for the time



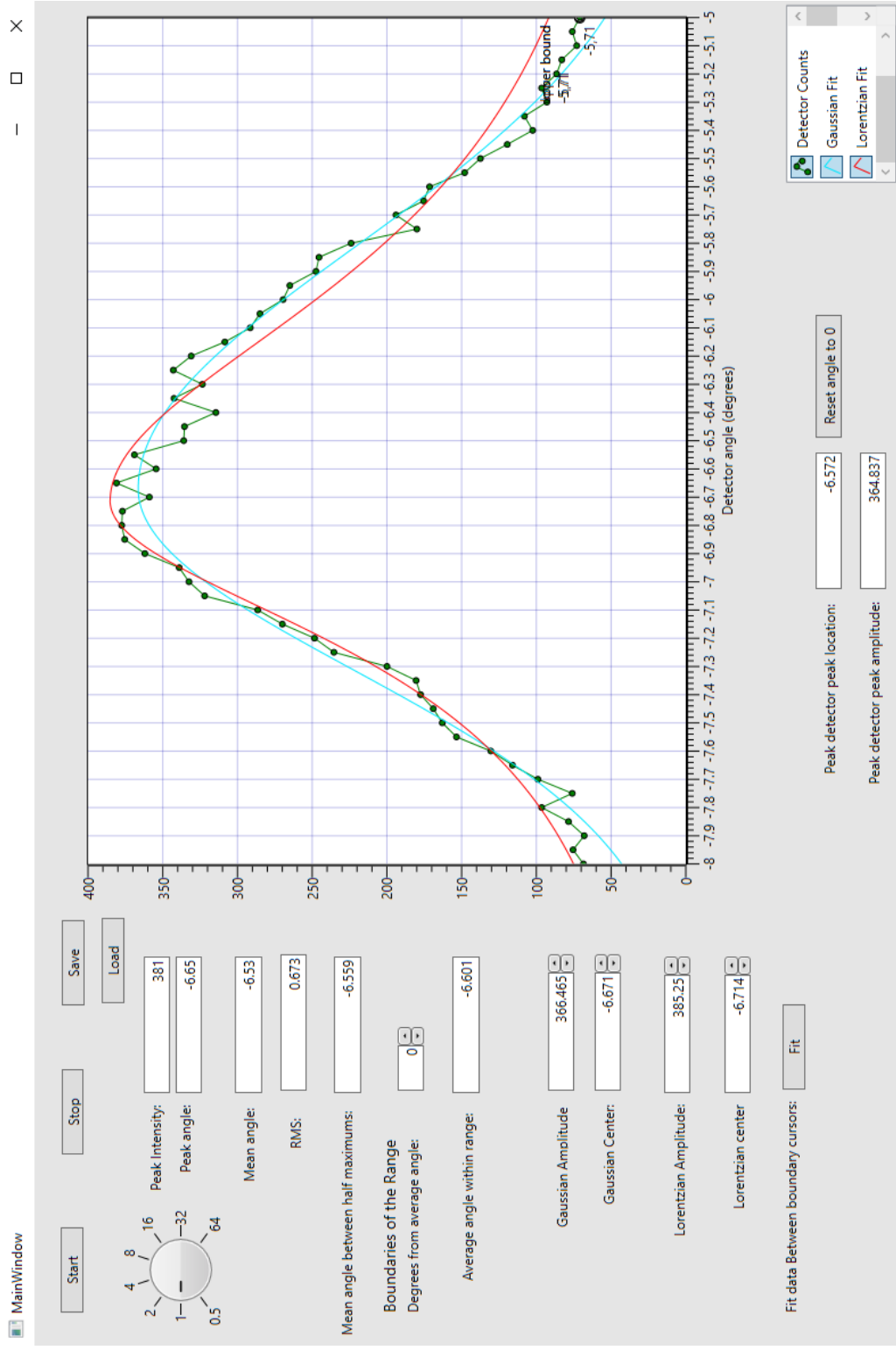


Figure 6: A screen capture of a detector scan from  $-8$  to  $-5$  degrees in increments of  $0.05$  degrees, showing the current set of analysis methods that are being tested. Each data point is plotted in green, while the Gaussian fit is shown in blue and the Lorentzian fit in red.

dependence of the plasma source, therefore any variations seen in the reflectance should be due entirely to the angle of the sample, and the data can be interpreted accordingly.

## 5 Milestones

- Developed the controls for moving the fabrication box and added these controls to the octopus program.
- Cleaned up the program for the evaporator and added these controls to the octopus program.
- Finished developing the code responsible for moving the detector and sample motors in the  $\theta - 2\theta$  scan process.
- Created a separate program that monitors and records the voltage, pressure and current of a selected plasma source, and added the controls allowing the user to choose the plasma source to monitor to the existing plasma monitor within the Octopus program.
- Created a help menu that gives a detailed description of the function of each tab in the Octopus program.
- Adjusted the existing detector harness to emulate the effect of plasma source and the position of the detector on the value of the count.
- Completed the code for analyzing the  $\theta - 2\theta$  data and accounting for the time dependence of the plasma source, excluding the code responsible for determining a single count value from a detector scan.
- Created a new tab in the Octopus program responsible for scanning the detector across the beam and analyzing the resulting data.

## 6 Future Plans

Currently, research is still focused on using the detector scan program to narrow the possibilities to a single method that gives us consistent results. This method will then be implemented in the in the  $\theta - 2\theta$  scans. Once this has been decided, the  $\theta - 2\theta$  scan program is ready to be tested with the actual equipment.

## References

- [1] Benjamin D. Smith, “Reflectance Measurements of Two Thin Film Materials in the UV.” Senior Thesis, Brigham Young University, (2015).
- [2] David D. Allred and R. Steven Turley, *Getting to the Best Broadband Mirror Coatings Possible for Space: Answering some key basic science questions so significant Far-UV and EUV performance can be added to future broadband space telescopes*. Brigham Young University, internal report, (April 2017).
- [3] <https://asd.gsfc.nasa.gov/luvoir> (Accessed 15 Aug 2017).
- [4] David Windt, <http://www.rxollc.com> (Accessed 17 Aug 2017).